FEBS Letters 580 (2006) 1360–1364

The μO-conotoxin MrVIA inhibits voltage-gated sodium channels by associating with domain-3

Stefan Zorn[a,1], Enrico Leipold[a,1], Alfred Hansel[a], Grzegorz Bulaj[b], Baldomero M. Olivera[b], Heinrich Terlau[c], Stefan H. Heinemann[a,*]

[a] *Institute of Molecular Cell Biology, Research Unit "Molecular and Cellular Biophysics", Medical Faculty of the Friedrich Schiller University Jena, Drackendorfer Str. 1, D-07747 Jena, Germany*
[b] *Department of Biology, University of Utah, Salt Lake City, UT 84112, USA*
[c] *Institute of Experimental and Clinical Pharmacology and Toxicology, University of Lübeck, Ratzeburger Allee 160, 23538 Lübeck, Germany and Max Planck Institute for Experimental Medicine, Molecular and Cellular Neuropharmacology Group, 37075 Göttingen, Germany*

Received 5 January 2006; accepted 12 January 2006

Available online 26 January 2006

Edited by Maurice Montal

Abstract **Several families of peptide toxins from cone snails affect voltage-gated sodium (Na_V) channels: μ-conotoxins block the pore, δ-conotoxins inhibit channel inactivation, and μO-conotoxins inhibit Na_V channels by an unknown mechanism. The only currently known μO-conotoxins MrVIA and MrVIB from *Conus marmoreus* were applied to cloned rat skeletal muscle ($Na_V1.4$) and brain ($Na_V1.2$) sodium channels in mammalian cells. A systematic domain-swapping strategy identified the C-terminal pore loop of domain-3 as the major determinant for $Na_V1.4$ being more potently blocked than $Na_V1.2$ channels. μO-conotoxins therefore show an interaction pattern with Na_V channels that is clearly different from the related μ- and δ-conotoxins, indicative of a distinct molecular mechanism of channel inhibition.**

Keywords: Sodium channel; Conotoxin; Neurotoxin; Patch clamp; Channel block; Pain

1. Introduction

Voltage-gated sodium channels (Na_V channels) are key elements for the generation of action potentials of electrically excitable cells [1]. The fast activation and inactivation of these channels is crucial for shaping the upstroke depolarization of an action potential. A variety of neurotoxins from different organisms act on Na_V channels and affect the cellular excitability (e.g., [2–5]). Several families of peptide toxins from the venom of cone snails modulate Na_V channels: μ-conotoxins and μO-conotoxins block channel conductance, whereas δ-conotoxins increase currents by inhibiting inactivation [6].

The μ-conotoxins "block" the channel by interacting with receptor site-1, which is the binding site of the classical Na_V channel blockers tetrodotoxin (TTX) and saxitoxin (STX) (review: [7]). μ-Conotoxins belong to the M-superfamily, δ- and μO-conotoxins to the O-superfamily of conopeptides. The latter have a cysteine backbone, which is different from the one of μ-conotoxins but similar to that of ω-conotoxins, which interact with voltage-gated Ca^{2+} channels. δ-Conotoxins interact with receptor site-6 of Na_V channels. Our recent study [8], however, showed that δ-conotoxins, like scorpion α-toxins or sea anemone toxins, interact with the S3/4 linker of domain-4. Hence, receptor site-3 and site-6 seem to be overlapping structural entities.

Despite their structural similarities to δ-conotoxins, μO-conotoxins block sodium current and apparently do not slow inactivation [9]. In addition, they seem to have blocking potency for calcium channels [10]. Competition studies with labeled STX suggest that μO-conotoxins do not block Na_V channels by interacting with receptor site-1 [11]. The site of action and the mechanism through which μO-conotoxins affect Na_V channels are still unknown.

There is considerable interest in elucidating such mechanisms because uniquely, μO-conotoxins seem to block TTX-resistant sodium channels effectively ($Na_V1.8$ [12]). These channels are expressed in peripheral nerves, and their specific suppression may provide an analgesic strategy. Systematic studies are, however, hampered by the complication of expressing $Na_V1.8$ channels in mammalian cells. In addition, thus far no marked subtype specificity of the toxins that would allow for a systematic search for binding sites or molecular mechanisms of channel modulation has been shown.

2. Materials and methods

2.1. Construction of channel chimeras

The rat channel isoforms $Na_V1.2$ (X03639 [13]) and $Na_V1.4$ (M26643.1 [14]) were expressed from the vectors pCIneo and pcDNA3, respectively. Using PCR-based site-directed mutagenesis, three silent mutations (C3121G, G3123A, and C3868T) were introduced into the $Na_V1.4$ ORF to generate an *Nhe*I restriction site at position 3121 and a *Cla*I site at position 3864. These two restriction sites, an endogenous *Bsi*WI site (position 1329), a *Bst*EII site at the 3′ end, and an *Xba*I site at the 5′ end of the channel-coding gene were used to extract DNA fragments coding for the four channel domains (domain-1: *Bst*EII/*Bsi*WI, domain-2: *Bsi*WI/*Nhe*I, domain-3: *Nhe*I/*Cla*I, domain-4: *Cla*I/*Xba*I). DNA fragments coding for the homologous parts of $Na_V1.2$ were subcloned into the pGEMT vector (Promega Corp., Madison, USA) with primers that introduced restriction sites for *Bsi*WI, *Nhe*I, *Cla*I, *Bst*EII,

*Corresponding author. Fax: +49 3641 9 32 56 82.
E-mail address: Stefan.H.Heinemann@uni-jena.de (S.H. Heinemann).

[1] These authors contributed equally.

Abbreviations: Na_V channels, voltage-gated sodium channels; TTX, tetrodotoxin; STX, saxitoxin

0014-5793/$32.00
doi:10.1016/j.febslet.2006.01.057

and *Xba*I in homologous positions. The four $Na_V1.2$ fragments were introduced into $Na_V1.4$ resulting in four chimeras in which individual domains of $Na_V1.4$ are replaced by those of $Na_V1.2$: 2444 (domain-1), 4244 (domain-2), 4424 (domain-3), and 4442 (domain-4). In addition, we generated mutants in the background of wild-type $Na_V1.4$ ("44p4": E1251N, K1252V, E1254L, H1257K, and V1260D) and $Na_V1.2$ ("22p2": N1436E, V1437K, L1439E, K1442H, and D1445V) channels.

2.2. Toxin synthesis

MrVIA/B were synthesized using a modification of a method described previously [9]. The peptides were assembled on an automatic peptide synthesizer using 9-fluorenylmethoxycarbonyl (Fmoc) chemistry on a preloaded Fmoc-Val-Wang resin. It was removed from the resin by a 3-h treatment with reagent K and precipitated with cold methyl-tert-butyl ether (MTBE) chilled to −20°C. The precipitate was washed four times with cold MTBE. A reversed-phase HPLC purification of a reduced peptide was performed using a preparative diphenyl column (Vydac, model 219TP510) with a linear gradient of 90% acetonitrile/0.1% TFA in water, ranging from 30% to 90%. The first oxidation step was carried out by mixing the following reaction components (final concentrations in parentheses): isopropanol (30%), water, Tris–HCl buffer, pH 8.7 (100 mM), EDTA (1 mM), GSSG (1 mM), GSH (2 mM). The reaction was quenched with formic acid (1%) and then separated on the preparative diphenyl HPLC column. The second folding step included formation of the disulfide bond between Cys9 and Cys25 and was carried out in 40% acetonitrile, and 1 mM iodine, 2.5% TFA for 20 min at room temperature. The oxidation product was purified on the diphenyl preparative HPLC column, as described for the linear form.

2.3. Electrophysiological measurements

Cultivation and transfection of HEK 293 cells as well as whole-cell voltage clamp experiments and toxin application were performed as described previously [15]. The patch pipettes contained (mM): 35 NaCl; 105 CsF; 10 EGTA; and 10 HEPES (pH 7.4 with CsOH). The bath solution contained (mM): 150 NaCl; 2 KCl, 1.5 $CaCl_2$; 1 $MgCl_2$; and 10 HEPES (pH 7.4 with NaOH). The toxins were stored frozen in extracellular bath solution additionally containing 1 mg/ml BSA.

Channel activation was assayed by test depolarizations from −80 to +60 mV at an interval of 10 s. The peak currents were fit with a Hodgkin–Huxley activation formalism involving three activation gates and a single-channel characteristic according to the Goldman–Hodgkin–Katz equation:

$$I_{\mathrm{peak}}(V) = \frac{I_{\max}}{\left(1 + \mathrm{e}^{-(V - V_{\mathrm{m}})/k_{\mathrm{m}}}\right)^3}$$
$$I_{\max} = \Gamma V \frac{1 - \mathrm{e}^{-(V - E_{\mathrm{rev}})/25\,\mathrm{mV}}}{1 - \mathrm{e}^{-V/25\,\mathrm{mV}}} \quad (1)$$

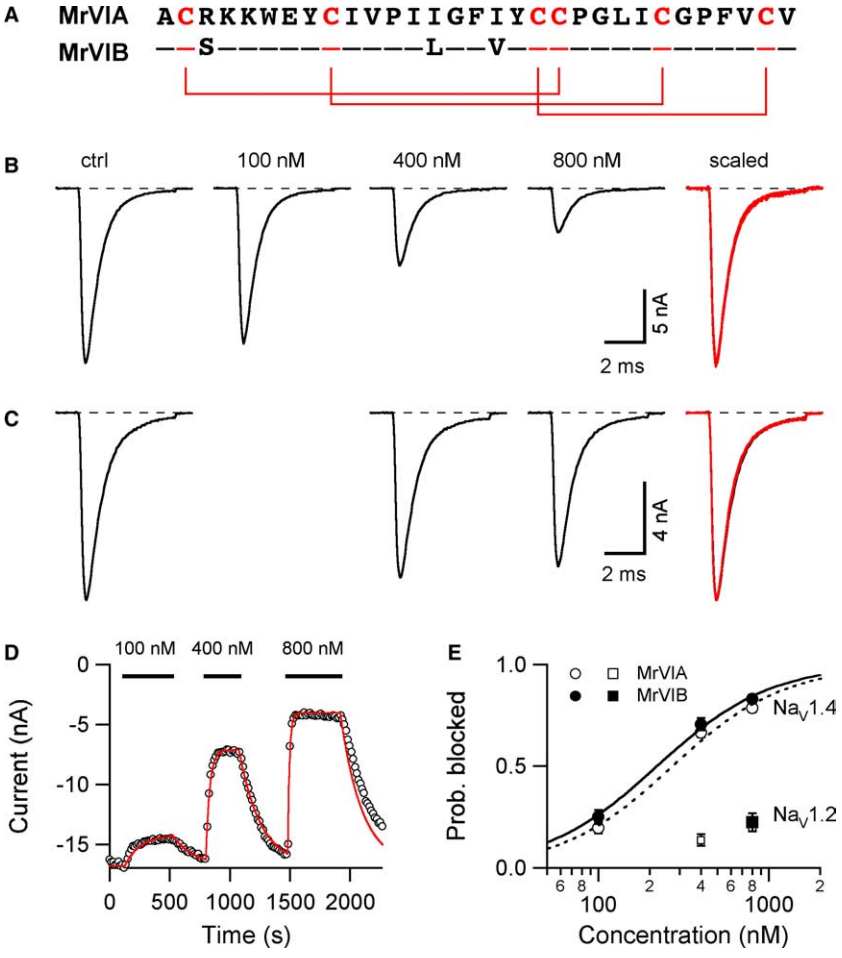

Fig. 1. Block of $Na_V1.4$ channels by MrVIA and MrVIB. (A) Alignment of MrVIA and MrVIB indicating the disulfide bridge structure. (B) Current responses to depolarizations to −20 mV for $Na_V1.4$ channels expressed in HEK 293 cells under control conditions and after application of the indicated concentrations of MrVIA. The panel on the right shows the traces recorded in the presence of toxin superimposed to the control and scaled in magnitude by the factors 1.135 (100 nM), 2.30 (400 nM), and 4.01 (800 nM). (C) A similar experiment as in (B) but with $Na_V1.2$ channels. The presence of 400 and 800 nM MrVIA resulted in weak current block (scaling factors of 1.13 and 1.22, respectively). (D) Pulses to −20 mV were elicited every 30 s and the peak current is plotted here as a function of time under the indicated applications of MrVIA. The superimposed curve is a fit to the data assuming that the block obeys an on-rate of $1/(\tau = 12.800\ \mathrm{s/conc[nM]})$ and an off-rate of $1/(\tau = 180\ \mathrm{s})$. (E) Concentration–response curves for blocking $Na_V1.4$ channels by MrVIA (open) and MrVIB (filled circles). The continuous curves are Hill fits (Eq. (3)). The squares indicate data for $Na_V1.2$ channels.

where V_m is the voltage of half-maximal gate activation and k_m the corresponding slope factor. Γ is the maximal conductance of all channels and E_{rev} the reversal potential.

Voltage dependence of fast inactivation was evaluated by measuring current at −20 mV after 500-ms conditioning pulses ranging from −140 to −30 mV (repetition interval of 15 s). The peak current versus the conditioning voltage was described with a Boltzmann function:

$$I(V) = \frac{I_{min}}{(1 + e^{-(V-V_h)/k_h})} \quad (2)$$

with the half-maximal inactivation voltage V_h and the corresponding slope factor k_h.

Toxin dependence of current inhibition was measured under repetitive pulsing to −20 mV at an interval of 15 s. The dose dependence for toxin-induced current reduction was described with the Hill equation:

$$I/I_c = \frac{1}{1 + \left(\frac{conc}{IC_{50}}\right)^h} \quad (3)$$

where h is the Hill coefficient and *conc* the toxin concentration. IC_{50} provides a measure for the concentration of half-maximal channel inhibition. Data points were weighted according to the standard error of the mean; error estimates for IC_{50} values were obtained from these fits with the IgorPro program (WaveMetrics, Lake Oswego, OR, USA). The holding potential was −120 mV for all experiments.

Data acquisition and analysis were performed with PatchMaster and FitMaster software, respectively (HEKA Elektronik, Lambrecht, Germany). All data were presented as means ± S.E. of the mean (n = number of independent experiments).

3. Results and discussion

3.1. Block of rNa$_V$1.4 and rNa$_V$1.2 channels by μO-conotoxins

Rat $Na_V1.4$ channels were expressed in HEK 293 cells and the effects of the μO-conotoxins MrVIA and MrVIB (Fig. 1A) were assayed under whole-cell patch clamp conditions. As shown in Fig. 1B, application of increasing concentrations of MrVIA reduced the current magnitude when channel activity was measured under repetitive pulses to −20 mV. The time course of the remaining current did not significantly differ from the control as shown in the scaled-up version in the rightmost panel of Fig. 1B. Fig. 1C shows similar experiments performed with $Na_V1.2$ channels. Even 800 nM MrVIA exhibits only a very small blocking effect on the evoked currents. Furthermore, the time course of the currents in the presence of the toxin is not altered either. Similar results were obtained with MrVIB. Thus, MrVIA and MrVIB, unlike the structurally related δ-conotoxins, do not affect the time course of channel activation or inactivation. In Fig. 1D, the time course of peak currents is shown for the indicated applications of MrVIA. The current is blocked rapidly and reversibly. The continuous curve is a data fit assuming a block on-rate of 780/(ms nM) and an off-rate of 5.5/ms. Therefore, the on-rate is roughly a linear function of toxin concentration and the off-rate seems to be independent of toxin concentration indicating a simple bimolecular reaction. The potency of the toxins to reduce the $Na_V1.4$-mediated current amplitude was estimated by compiling concentration–response curves (Fig. 1E), described by a Hill equation (Eq. (3)), yielding IC_{50}-values of 265 ± 16 and 222 ± 18 nM, and Hill coefficients of 1.32 ± 0.10 and 1.31 ± 0.12 for MrVIA and MrVIB, respectively. Thus, the toxins display an indistinguishable potency to block $Na_V1.4$ channels. A Hill coefficient close to unity suggests that one toxin molecule might be sufficient for channel block.

The difference of toxin effect on muscle and brain channels was not expected because Safo et al. [16] reported that MrVIA did not discriminate well between rNa$_V$1.4 (IC_{50} 438 nM), rNa$_V$1.2 (532 nM), and rNa$_V$1.7 (345 nM) when the channels were expressed in *Xenopus* oocytes. Presently we do not know the differences between those results and ours obtained in HEK 293 cells. Nevertheless, our experiments clearly demonstrate that MrVIA has a preference for $Na_V1.4$ over $Na_V1.2$ channels. This preference and the absolute potency is the same for MrVIA and MrVIB, indicating that the minor sequence differences between the two toxins (see Fig. 1A) have no effect on the toxin interaction with the mammalian channel types assayed.

The current reduction induced by the MrVI toxins did not depend on the magnitude of membrane depolarization. As shown in Fig. 2A, 400 nM MrVIA reduced the peak current of $Na_V1.4$ channels to the same extent throughout a complete current–voltage recording. In addition, no strong shift in steady-state inactivation is observed in the presence of toxins (Fig. 2B). For wild-type $Na_V1.4$ channels V_h was −75.5 ± 1.8 mV before and −82.2 ± 1.9 mV (n = 6) after application of 400 nM MrVIA. Thus, since the holding voltage used in this study was −120 mV throughout, we can safely exclude a shift of steady-state inactivation as cause for μO-conotoxin-induced current block. The averaged parameters characterizing channel activation and inactivation are listed in Table 1.

3.2. Identification of domain-3 as a major interaction site

The difference in the toxin effect on $Na_V1.4$ over $Na_V1.2$ channels provide the opportunity to systematically search for domains in the channel protein important for toxin action. This is particularly intriguing, as currently there is no information on the channel binding sites occupied by μO-conotoxins. For an initial screening we generated chimeras between $Na_V1.4$ and $Na_V1.2$ channels in which the majority of the

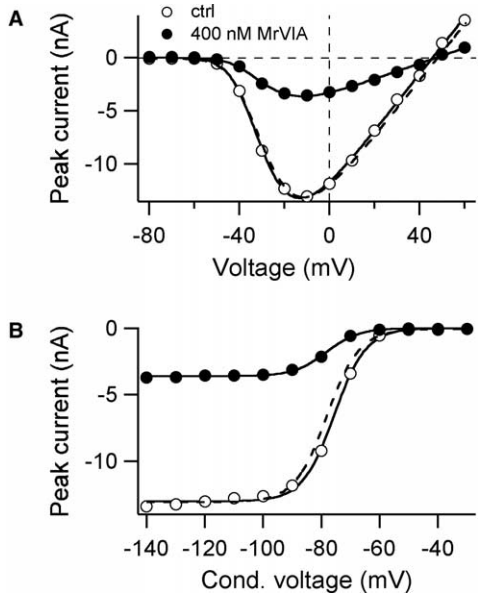

Fig. 2. Voltage-dependent parameters. (A) Current–voltage relationship for $Na_V1.4$ channels under control conditions (open circles) and after application of 400 nM MrVIA (filled circles). The continuous curves are data fits according to a Hodgkin and Huxley activation model (Eq. (1)). The broken continuous curve superimposed to the control data is the fit resulting from the toxin data, scaled by a factor of 3.6. (B) Steady-state inactivation curve (Eq. (2)) for the same cell as in (A) and using the same symbols.

Table 1
Steady-state activation and inactivation parameters as well as current block by 400 nM MrVIA characterizing wild-type channels and channel chimeras

Channel	V_m (mV)	k_m (mV)	n	V_h (mV)	k_h (mV)	n	% Block	n
rNa$_V$1.4 (4444)	−45.6 ± 1.9	10.2 ± 0.7	10	−75.1 ± 1.9	5.0 ± 0.2	10	68.4 ± 1.1	22
rNa$_V$1.2 (2222)	−39.2 ± 3.3	12.2 ± 0.2	5	−72.6 ± 3.0	4.8 ± 0.1	5	13.6 ± 2.8	8
2444	−45.7 ± 1.1	10.0 ± 0.3	4	−73.9 ± 0.8	5.0 ± 0.2	5	62.8 ± 2.6	9
4244	−42.9 ± 2.1	10.4 ± 0.3	7	−75.9 ± 1.7	5.2 ± 0.1	7	67.9 ± 4.9	11
4424	−41.5 ± 1.8	8.7 ± 0.9	5	−71.5 ± 0.7	4.9 ± 0.2	5	16.2 ± 1.5	5
4442	−49.3 ± 2.4	10.4 ± 0.6	6	−79.7 ± 1.8	5.3 ± 0.1	6	71.0 ± 2.6	9
44p4	−46.0 ± 1.0	9.2 ± 0.3	8	−73.3 ± 0.9	4.6 ± 0.1	8	19.9 ± 3.0	8
22p2	−44.0 ± 1.3	12.4 ± 0.5	4	−76.4 ± 1.4	4.9 ± 0.1	4	46.3 ± 3.9	6

V_m and k_m values determined from current–voltage relationships according to Eq. (1), V_h and k_h values from steady-state inactivation protocols according to Eq. (2), and the percentage of current block upon application of 400 nM MrVIA.

construct was from Na$_V$1.4: Individual domains were exchanged between the two channel isoforms yielding the constructs 2444, 4244, 4424, and 4442 as depicted in Fig. 3A. All domain chimeras were assayed for the effect of 400 nM MrVIA yielding strong current block, i.e. a Na$_V$1.4 phenotype, in all chimeras but 4424. This result is somewhat surprising as this is the first case in which domain-3 is the major determinant for the discrimination of channel isoforms by neurotoxins.

All chimeras were also investigated with respect to the voltage dependence of activation and fast inactivation. As listed in Table 1, none of the chimeras dramatically deviated from the wild-type Na$_V$1.4 channel indicating that the observed differences in toxin effect are not due to altered gating characteristics introduced by formation of the chimeras.

To further narrow down a potential interaction site between μO-conotoxins and Na$_V$ channels, we constructed another chimera in which only the C-terminal part of the pore loop (SS2) of Na$_V$1.2 was transferred into Na$_V$1.4 (Fig. 3A, bottom). This part of the pore loop only contains five differences between the channel isoforms. The assay with 400 nM MrVIA also yielded a strong reduction in the blocking potency (Fig. 3B, bottom) suggesting that SS2 plays a major role in the binding of

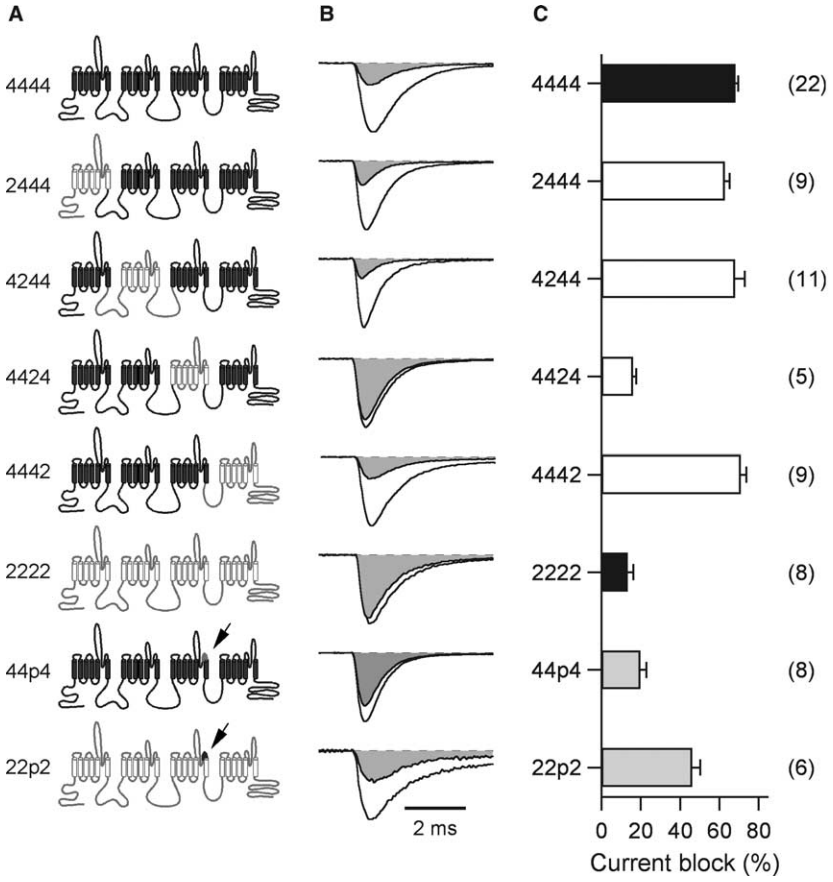

Fig. 3. Chimeras and assay of toxin effects. (A) Cartoons illustrating the construction of channel chimeras. Parts originating from Na$_V$1.4 are shown in black, parts from Na$_V$1.2 in grey. In chimeras "44p4" and "22p2" the SS2 pore loops of domain-3, indicated by the arrows, have been exchanged. (B) Superimposed current traces of the corresponding channel constructs obtained upon depolarization to −20 mV under control conditions and after application of 400 nM MrVIA (grey shading). (C) Average block of peak current after application of 400 nM MrVIA for the indicated channel constructs. The error bars denote S.E.M. values and the numbers in parentheses the numbers of experiments.

μO-conotoxins to the channels. Since a reduction of the toxin effect induced by mutagenesis at five positions may be rather accidental, we generated the reverse chimera, i.e. a $Na_V1.2$ channel with the SS2 pore loop of domain-3 from $Na_V1.4$. This chimera was blocked much more efficiently than the corresponding wild-type $Na_V1.2$ (Fig. 3, last row), clearly showing that the identified region is a major determinant for the action of μO-conotoxins. These data therefore add a new molecular entity to the interaction sites of biologically active neurotoxins on Na_V channels.

μO-conotoxins, although they exhibit structural similarities to δ-conotoxins, do not affect inactivation of Na_V channels, but instead block the channel conductance. This effect seems similar to that of μ-conotoxins. However, binding studies with radiolabeled STX indicated that μO-conotoxin MrVIA is not interacting with receptor site-1 of the channel [11]. In contrast to μ-conotoxins, which make multiple couplings to the pore loop of different channel domains of the Na_V channel α-subunit [6,17], our data indicate that μO-conotoxins do block Na_V channels by interacting mainly with the C-terminal part of the pore loop of domain-3. The pore regions of the domains 1, 2, and 4 seem to be less important for μO-conotoxin binding, at least they are not crucial for the difference between $Na_V1.2$ and $Na_V1.4$ channels. The pore loop of domain-3, however, also seems to be important for the binding of scorpion β-toxins [18,19].

3.3. Potential value of μO-conotoxins

The differences of MrVIA effects on $Na_V1.4$ and $Na_V1.2$ channels could be used to identify potential interaction sites at the channel protein. However, higher concentrations of MrVIA also affect $Na_V1.2$ channels and they even seem to affect Ca_V channels [10]. Therefore, the overall specificity of μO-conotoxins seems to be rather weak and not comparable to the specificity observed for structurally related ω-conotoxins that block Ca_V channels. Since μO-conotoxins also block TTX-resistant $Na_V1.8$ channels in dorsal root ganglia neurons involved in pain sensation [12], these peptides might be important tools for studying these channels. Furthermore, the known structure of μO-conotoxins [12] might serve as a starting point for developing substances that specifically block $Na_V1.8$ channels; this could be a major breakthrough for the development of new analgetics. The results presented in this study can pave the way for a deeper understanding of the specificity of μO-conotoxins towards different Na_V channel subtypes.

Acknowledgments: We thank A. Roßner and S. Arend for technical assistance, Dr. J. Trimmer for providing the coding sequence of $rNa_V1.4$ and Dr. M. Noda for $rNa_V1.2$. This work was supported by grants from the Deutsche Forschungsgemeinschaft (HE 2993/5, to S.H.H.) and NIH (Grant GM48677 to B.M.O.).

References

[1] Catterall, W.A. (2000) From ionic currents to molecular mechanisms: the structure and function of voltage-gated sodium channels. Neuron 26, 13–25.
[2] Gordon, D. (1997) Na channels as targets for neurotoxins: mode of action and interaction of neurotoxins with receptor sites on Na channels in: Toxins and Signal Transduction (Lazarowici, P. and Gutman, Y., Eds.), Cellular and Molecular Mechanisms of Toxin Action Series, pp. 119–149, Harwood Press, Amsterdam.
[3] Zlotkin, E. (1999) The insect voltage-gated sodium channel as target of insecticides. Annu. Rev. Entomol. 44, 429–455.
[4] Cestèle, S. and Catterall, W.A. (2000) Molecular mechanisms of neurotoxin action on voltage-gated sodium channels. Biochimie 92, 883–892.
[5] Catterall, W.A. (2002) Molecular mechanisms of gating and drug block of sodium channels. Novartis Found. Symp. 214, 206–225.
[6] Terlau, H. and Olivera, B.M. (2004) *Conus* venoms: a rich source of novel ion channel-targeted peptides. Physiol. Rev. 84, 41–68.
[7] French, R.J. and Terlau, H. (2004) Sodium channel toxins–receptor targeting and therapeutic potential. Curr. Med. Chem. 11, 3053–3064.
[8] Leipold, E., Hansel, A., Olivera, B.M., Terlau, H. and Heinemann, S.H. (2005) Molecular interaction of δ-conotoxins with voltage-gated sodium channels. FEBS Lett. 579, 3881–3884.
[9] McIntosh, J.M., Hasson, A., Spira, M.E., Gray, W.R., Li, W., Marsh, M., Hillyard, D.R. and Olivera, B.M. (1995) A new family of conotoxins that blocks voltage-gated sodium channels. J. Biol. Chem. 270, 16796–16802.
[10] Fainzilber, M., van der Schors, R., Lodder, J.C., Li, K.W., Geraerts, W.P. and Kits, K.S. (1995) New sodium channel-blocking conotoxins also affect calcium currents in *Lymnaea* neurons. Biochemistry 34, 5364–5371.
[11] Terlau, H., Stocker, M., Shon, K.J., McIntosh, J.M. and Olivera, B.M. (1996) μO-conotoxin MrVIA inhibits mammalian sodium channels, but not through site I. J. Neurophysiol. 76, 1423–1429.
[12] Daly, N.L., Ekberg, J.A., Thomas, L., Adams, D.J., Lewis, R.J. and Craik, D.J. (2004) Structures of μO-conotoxins from *Conus marmoreus*. Inhibitors of tetrodotoxin (TTX)-sensitive and TTX-resistant sodium channels in mammalian sensory neurons. J. Biol. Chem. 279, 25774–25782.
[13] Noda, M., Ikeda, T., Suzuki, H., Takeshima, H., Takahashi, T., Kuno, M. and Numa, S. (1986) Expression of functional sodium channels from cloned cDNA. Nature 322, 826–828.
[14] Trimmer, J.S., Cooperman, S.S., Tomiko, S.A., Zhou, J.Y., Crean, S.M., Boyle, M.B., Kallen, R.G., Sheng, Z.H., Barchi, R.L., Sigworth, F.J., Goodman, R.H., Agnew, W.S. and Mandel, G. (1989) Primary structure and functional expression of a mammalian skeletal muscle sodium channel. Neuron 3, 33–49.
[15] Chen, H., Gordon, D. and Heinemann, S.H. (1999) Modulation of cloned skeletal muscle Na channels by the scorpion toxins Lqh II, Lqh III, and LqhαIT. Pflügers Arch. 439, 423–432.
[16] Safo, P., Rosenbaum, T., Shcherbatko, A., Choi, D.-Y., Han, E., Toledo-Aral, J.J., Olivera, B.M., Brehm, P. and Mandel, G. (2000) Distinction among neuronal subtypes of voltage-activated sodium channels by μ-conotoxin PIIA. J. Neurosci. 20, 76–80.
[17] Li, R.A., Tsushima, R.G., Kallen, R.G. and Backx, P.H. (1997) Pore residues critical for μ-CTX binding to rat skeletal muscle Na^+ channels revealed by cysteine mutagenesis. Biophys. J. 73, 1874–1884.
[18] Gordon, D., Moskowitz, H., Eitan, M., Warner, C., Catterall, W.A. and Zlotkin, E. (1992) Localization of receptor sites for insect-selective toxins on sodium channels by site-directed antibodies. Biochemistry 31, 7622–7628.
[19] Cestèle, S., Qu, Y., Rogers, J.C., Rochat, H., Scheuer, T. and Catterall, W.A. (1998) Voltage sensor-trapping: enhanced activation of sodium channels by β-scorpion toxin bound to the S3-S4 loop in domain II. Neuron 21, 919–931.